



Evaluation of regional climate simulations over the Great Lakes region driven by three global data sets

Shiyuan Zhong^{a,*}, Xiuping Li^{b,1}, Xindi Bian^{c,2}, Warren E. Heilman^c,
L. Ruby Leung^{d,3}, William I. Gustafson Jr.^{d,4}

^a Department of Geography and Center for Global Climate Change and Earth Observations, Michigan State University, East Lansing, MI 48824, USA

^b College of Water Sciences, Beijing Normal University, Beijing 100875, China

^c USDA Forest Service, Northern Research Station, East Lansing, MI 48823, USA

^d Pacific Northwest National Laboratory, Richland, WA 99354, USA

ARTICLE INFO

Article history:

Received 3 March 2011

Accepted 3 March 2012

Available online 24 April 2012

Communicated by Ram Yerubandi

Keywords:

Regional climate model

Climate modeling of the Great Lakes region

MM5

ABSTRACT

The performance of regional climate simulations is evaluated for the Great Lakes region. Three 10-year (1990–1999) current-climate simulations are performed using the MM5 regional climate model (RCM) with 36-km horizontal resolution. The simulations employed identical configuration and physical parameterizations, but different lateral boundary conditions and sea-surface temperatures derived from the NCEP Global Reanalysis and output from the CCSM3 and GISS general circulation models (GCMs). The simulation results are compared to the North American Regional Reanalysis (NARR). The three RCM simulations appeared to be more accurate in winter and least accurate in summer, and more accurate aloft than near the surface. The reanalysis-constrained simulation adequately captured the spatial distribution and seasonal cycle of the observed surface-air temperature and precipitation, but it produced consistently across all seasons a cold bias that is generally larger over the lakes than over land and a wet bias due to an overestimation of non-convective precipitation. The simulated seasonal cycle of moisture–flux convergence over the region was in very good agreement with NARR. The two GCM-driven runs adequately simulated the spatial and seasonal variation of temperature, but overestimated cold-season precipitation and underestimated summer precipitation, reversing the observed annual precipitation cycle. The GISS-driven run failed to simulate the prevailing low-level flow and moisture convergence patterns. All three RCM simulations successfully captured the impact of the Great Lakes on the region's climate, especially on winter precipitation, a significant improvement over coarse-resolution GCM simulations over the region.

© 2012 International Association for Great Lakes Research. Published by Elsevier B.V. All rights reserved.

Introduction

As the largest fresh water source in the world, the North American Great Lakes region represents a major resource for various water usages (e.g., drinking, irrigation, shipping, ecological habitats, hydro-electric, and recreation) and plays an integral role in the U.S. and Canadian economy. The strong link between the Great Lakes water level and climate conditions makes the Great Lakes region particularly susceptible to the effect of global warming. According to the U.S.

National Assessment of Climate Change (NACC), the average temperature in the Great Lakes region is expected to rise by 2–4 °C by the end of the 21st century, which could have a profound impact on the region, as the warmer climate may reduce water supplies and increase water demand within the region. A warmer climate could also reduce water supplies in other parts of the United States, increasing the pressure to divert Great Lakes water to other regions. Hall and Stuntz (2008) examined what a changing climate will mean for the Great Lakes region, including possible lowering of water levels, changes in shoreline, reduction in ground water supply, and impacts on fisheries and wildlife. Mortsch et al. (2000) provided a review of the current state of knowledge on climate change and the response of the climate and hydrologic systems to a changing atmosphere. The review presented historical trends in and the impact of climate change on temperature, precipitation, evapotranspiration, runoff, and Great Lakes water levels. Hayhoe et al. (2010) applied statistical downscaling to a large number of global climate simulations and summarized the regional climate change in the Chicago and Great Lakes region.

* Corresponding author at: 116 Geography Building, Michigan State University, East Lansing, MI 48823, USA. Tel.: +1 517 432 4743.

E-mail addresses: zhongs@msu.edu (S. Zhong), lixiuping@bnu.edu.cn (X. Li), xbian@fs.fed.us (X. Bian), wheilam@fs.fed.us (W.E. Heilman), ruby.leung@pnl.gov (L.R. Leung), william.gustafson@pnl.gov (W.I. Gustafson).

¹ Tel.: +86 010 58801989.

² Tel.: +1 517 355 7740.

³ Tel.: +1 509 372 6182.

⁴ Tel.: +1 509 372 6110.

To date, various assessments on the potential impacts of global warming on the Great Lakes region have been based primarily on climate projections from General Circulation Models (GCMs) (Mortsch et al., 2000; Sousounis and Bisanz, 2000; Lofgren et al., 2002; Karl et al., 2009). Although GCM projections provide information on potential climate change for the region as a whole, they are unable to provide spatial details needed for many impact studies that are at regional or local scales. Most GCMs, with nominal horizontal resolution on the order of 150–300 km, are inadequate in resolving the lakes and shorelines and, consequently, are unable to represent the influence of the Great Lakes on the region's climate.

Regional climate models (RCMs) have emerged as an effective tool for dynamically downscaling coarse resolution GCM projections to the scales useful for regional climate predictions and climate impact assessments (Lettenmaier and Gan, 1990; Mearns et al., 1995; McGregor, 1997; Castro et al., 2005; Gustafson and Leung, 2007). In dynamical downscaling, regional or limited-area models are driven by large-scale boundary conditions, including winds, temperatures, water vapor, and sea surface temperatures, provided by GCMs or analysis products to simulate atmospheric circulations for a region at high spatial resolution (Giorgi and Mearns, 1999; Leung et al., 2003a; Roads et al., 2003). According to Giorgi and Marinucci (1996), RCMs allow for an improved representation of local and regional-scale circulations by better representations of topography and by increasingly realistic physical parameterizations. Comprehensive reviews of RCMs and regional climate modeling have been given by Wang et al. (2004) and Leung et al. (2003a).

Among the many advantages that RCMs have demonstrated over their global counterparts, improved prediction of quantitative precipitation, or more broadly, hydroclimate conditions, is perhaps the most significant advantage of RCMs over GCMs. This is especially true for regions of complex terrain. Miller and Kim (1996) successfully predicted quantitative precipitation and peak stream flows in the headwaters of the Russian River, California by driving an RCM with the National Centers for Environmental Prediction (NCEP) reanalyses. Leung and Ghan (1998, 1999) and Leung and Qian (2003) have demonstrated that the relative high resolution of RCMs improves precipitation and snowpack forecasts in the Pacific Northwest. Kim et al. (2000), Leung et al. (2003b), and Duffy et al. (2006) successfully applied different RCMs to simulate the observed hydroclimate in complex terrain regions of the western U.S. Even in regions of minimal orographic influence, the capability of RCMs in resolving important mesoscale dynamic processes can lead to a significant improvement in the simulation of hydrological cycles (Gutowski et al., 2004; Pan et al., 2004; Liang et al., 2004a, 2004b).

Despite the inadequacy of coarse-resolution GCMs in resolving the Great Lakes and their effects on the region's climate, only a few studies have applied RCMs to the Great Lakes region. Bates et al. (1993) evaluated the feasibility of applying the Pennsylvania State University–National Center for Atmospheric Research (NCAR) Mesoscale Model version 4 (MM4) coupled to a one-dimensional lake model to downscale large-scale weather forecasts over the Great Lakes region and found the results promising. Later, a two-year integration using this coupled regional model was performed, and the simulated climate of the Great Lakes region was shown to be in good agreement with observations (Bates et al., 1995). Goyette et al. (2000) evaluated the performance of a lake model coupled with the Canadian Regional Climate Model (CRCM) over eastern North America. The CRCM employed 45-km horizontal grid spacing and 10 vertical levels driven by the Canadian GCM output. The simulated seasonal evolution of surface temperature and ice cover in the Great Lakes as well as the snow accumulation patterns on downwind shores of the lakes from a five-year simulation were found to be realistic when compared with observations. Lofgren (2004) validated regional-scale simulations using the Coupled Hydrosphere–Atmosphere Research Model (CHARM) driven by historical data over the Great Lakes region. The CHARM simulation exhibits a small (less than 2 K) warm bias in surface temperature during winter and a cold bias in summer, and a

small (6.6%) positive bias in annual precipitation. The model captures the position of lake-effect precipitation, but the simulated land-water gradient is stronger than that observed.

This study is aimed at evaluating regional climate simulations of the Great Lakes region with a focus on hydroclimate conditions. The goal is to determine whether RCMs can serve as effective downscaling tools for climate impact and adaptation studies in this region.

The paper is organized as follows. The RCM used in the study and the experimental design and the dataset used for evaluating the RCM are described next, which is followed by results and discussions. The paper ends with a summary and a discussion of the current limitation and future work.

Data, model, and model simulations

The dataset employed for the RCM evaluation is the North American Regional Reanalysis (NARR) (Mesinger et al., 2006) produced by the National Centers for Environmental Prediction (NCEP). The NARR dataset is a long-term, dynamically consistent, high-resolution meteorology and hydrology gridded dataset for the North American continent. The data were produced using the NCEP mesoscale operational forecast model (Eta, 2003 frozen version) and its data assimilation system (EDAS). The horizontal grid spacing for the NARR data is 32 km, and there are 45 vertical layers in the atmosphere. The input observational data include all available surface and upper-air observations from various national and local networks. The reanalysis such as NARR is superior to operational analysis because the reanalysis datasets are able to assimilate quality-controlled data that may not be available in near-real time. The NARR dataset contains more than 180 surface, atmosphere, and soil variables at 8 times per day, starting from 1 January 1979 and continuing to the present.

Many previous studies have evaluated global or, in some cases, regional climate model simulations using the global counterpart of NARR, the NCEP–NCAR global reanalysis (Kalnay et al., 1996). In addition to its much finer resolution compared to its global counterpart that has a resolution of approximately 210 km, NARR has been enhanced with many additional and improved observational datasets, a more sophisticated land surface model, and improved data assimilation algorithms. Of particular interest to this study is its incorporation of daily precipitation observations that gives the NARR estimate of precipitation a higher degree of reliability. Another very important improvement in the NARR dataset related to the Great Lakes region is the assimilation of high resolution Great Lakes ice and temperature data that has improved the NARR's representation of climate over the Great Lakes region (Mesinger et al., 2006).

As an objectively analyzed gridded dataset that blends operational weather forecast model output with observational data through data assimilation, NARR data can be different from actual observations. Although studies have identified relatively large errors in the NARR data over areas of complex terrain such as the western U.S. (West et al. 2007) and in derived variables such as cloud products (Kennedy et al. 2011), the NARR data are found in general to be a good representation of the observed atmospheric state. This is especially true for regions over flat terrain such as the Great Plains of central U.S. (Mesinger et al., 2006; Kennedy et al. 2011) and the Great Lakes region (Li et al., 2010a, 2010b) as in this study. For the present work that requires a dataset that is long-term, relatively high in resolution, three-dimensional, and dynamically consistent in the atmosphere and hydrologic fields, NARR is currently the best available resource. We have compared NARR with observed surface and upper-air soundings in the Great Lakes region and the differences are generally small.

The climate simulations evaluated in this study were produced using the fifth-generation Penn State–NCAR Mesoscale Model (MM5; Grell et al., 1994). MM5 is a limited-area, nonhydrostatic, terrain-following sigma-coordinate, primitive equation model designed to

simulate or predict mesoscale atmospheric circulations. The model physics employed for the climate simulations include the Dudhia (1989) cloud radiation scheme, the Reisner et al. (1998) mixed-phase cloud microphysics scheme, the Kain and Fritsch (1990) cumulus parameterization, the Eta Model boundary-layer parameterization (Janjic, 1990), and a simple multilayer soil model. Various versions of MM5 (e.g., Leung and Ghan, 1998, 1999) have been used in the past for modeling regional climate. The model was found to be stable for long-term simulations and can produce the regional climatic features that are comparable to observations at the regional scale over the Pacific Northwest (e.g., Leung and Ghan, 1998) and the western U.S. (Leung et al., 2003b).

Three decade-long climate simulations of the current climate are produced for the continental United States. The first run employed lateral boundary conditions and sea-surface temperatures derived from the NCEP-NCAR global reanalysis dataset (Kalnay et al., 1996), and will be referred to as the “RCM-NCEP” run. The second simulation used lateral boundary conditions and sea-surface temperatures derived from the Community Climate System Model – Version 3 (CCSM3) (Collins et al., 2006) for the current climate, and will be referred to as the “RCM-CCSM” run. CCSM3 is a coupled ocean, land, and atmosphere global climate model with the atmospheric model applied at a horizontal grid spacing of T85 with 26 vertical levels. The CCSM3 output data for the current climate were downloaded from the NCAR Earth System Grid (www.earthsystemgrid.org). The third MM5 simulation of the current climate was driven by the National Aeronautics and Space Administration (NASA) Goddard Institute for Space Studies (GISS) general circulation model (Rind et al., 1999) output for the current climate, and will be referred to as the “RCM-GISS”. The GISS global climate simulation was described by Mickley et al. (2004), who applied the model at a horizontal resolution of 4° latitude by 5° longitude. The boundary conditions passed from the reanalysis/GCM datasets included large-scale temperature, atmospheric moisture, winds, and geopotential height, and are all interpolated horizontally and vertically to that of the MM5 model grid. MM5 does not include a lake model, so skin temperature over the Great Lakes were simply prescribed based on sea-surface temperature from the NCEP global reanalysis or GCM output interpolated from coast to coast to the location of the Great Lakes region. It should be noted that the NARR and NCEP reanalysis assimilate real-world data, while the GISS and CCSM do not. Therefore, the former two should yield results that line up with actual historical data, while the latter two won't and their results should merely be consistent with the boundary conditions of the global atmosphere for the time frame considered.

The MM5 simulations driven by the NCEP-NCAR global reanalysis (RCM-NCEP) and GISS (RCM-GISS) were described by Gustafson and Leung (2007). MM5 used a nested configuration with a coarse domain covering North America and the adjacent oceans at 108 km grid resolution and a fine domain covering the conterminous U.S. at 36 km grid resolution. RCM-CCSM followed the same model configuration for comparison. The simulation periods analyzed in this study include 1990–1999 for RCM-NCEP and RCM-CCSM and 1995–2004 for RCM-GISS. The MM5 model output data were archived every hour for analysis. Monthly, seasonal and annual means were averaged over the 10-year periods for each simulation to be representative of the current climate and compared with NARR for 1990–1999. The results of simulations are analyzed for the Great Lakes region defined here as 40°–50° N and 75°–94° W.

Results and discussions

Surface air temperature

Before we examine hydroclimate variables, we first examine the accuracy of the simulated surface-air temperatures. Temperature can indirectly influence the region's hydroclimate through its impact on

evaporation, atmospheric stability and vertical motion. Regional warming may also affect water quality and the supply and demand of water resources in the region.

Fig. 1 shows the spatial distribution of the 10-year seasonal mean surface-air temperature for spring (MAM), summer (JJA), autumn (SON), and winter (DJF) for the Great Lakes region. For all four seasons, the spatial temperature distribution across the Great Lakes region is dominated by a north-south gradient, with temperatures decreasing gradually from south to north. This spatial variation pattern is successfully simulated by all three RCM runs, but relatively large differences between the simulated and the NARR temperatures exist in some areas of the region. The RCM-NCEP exhibits a cold bias almost everywhere in the region, which appears to be more pronounced over the Great Lakes than over land areas. The RCM-CCSM and RCM-GISS simulated mean temperatures are in reasonably good agreement with the NARR temperatures, especially in spring and autumn. The surface-air temperatures over Lake Michigan and Lake Superior are overestimated by the RCM-GISS for all seasons and by the RCM-CCSM in summer. A warmer lake temperature would likely enhance the lake effect in the cold season while reduce the effect in warm season. The winter temperature pattern in the RCM-CCSM is similar to the RCM-NCEP temperature pattern with a cold bias across the region, while the RCM-GISS has a slight warm bias. Overall, the two GCM-driven runs have smaller bias values than the NCEP-driven run, with the RCM-CCSM slightly outperforming the RCM-GISS. The RCM-NCEP, however, appears to have better captured the spatial temperature distribution over the region.

To quantify the dependence of the NARR and the RCM surface temperature differences on seasons and surface types, monthly mean temperatures are obtained for all grid points, for the land points, and for the lake points, respectively, and the results are shown in Fig. 2. The domain-averaged monthly mean temperatures from NARR are below freezing from December through March and above freezing for the rest of the year. The same is true for the land- and lake-averaged monthly mean temperature except for November when land-averaged temperature dipped slightly below freezing while it is still above freezing over lake surfaces. From mid-spring through summer (April through August), the average NARR surface-air temperature is slightly warmer over land than over water, and the pattern is reversed from late fall to early spring (September through March).

All three RCM simulations adequately reproduced the month-to-month variation and the seasonal cycle. The RCM-NCEP exhibits a consistent cold bias throughout the year with larger bias over lakes than over land. The bias in RCM-CCSM, on the other hand, varies with season, with a cold bias from October through February and a warm bias during the rest of the year. The cold bias is slightly larger over water than over land, while the warm bias exhibits no systematic differences between land and lakes. The RCM-GISS temperatures are in closer agreement with the NARR compared to the other two runs and the biases appear to be independent of season and slightly larger over water. The overall larger bias over water in all three RCM runs reflects the errors introduced by prescribing lake skin temperatures based on nearby sea-surface temperatures. In contrast, with a sophisticated land-surface model, MM5 was able to capture the seasonal variability of surface temperature much better over land.

Compared to surface-air temperatures, the simulated upper-air temperatures are in much better agreement with the NARR data. Fig. 3 shows a comparison of 700 hPa seasonal mean temperature distributions across the region. The RCM-NCEP and RCM-CCSM adequately reproduce not only the observed spatial distributions but also the magnitudes. The RCM-GISS reproduces the magnitudes, but the spatial temperature distribution is dominated by a northeast-southwest gradient instead of a north-south gradient as seen in the NARR and the other two RCM runs, a possible reflection of larger errors in the GISS temperature distribution. The generally good agreement between the simulated and NARR upper-air temperatures

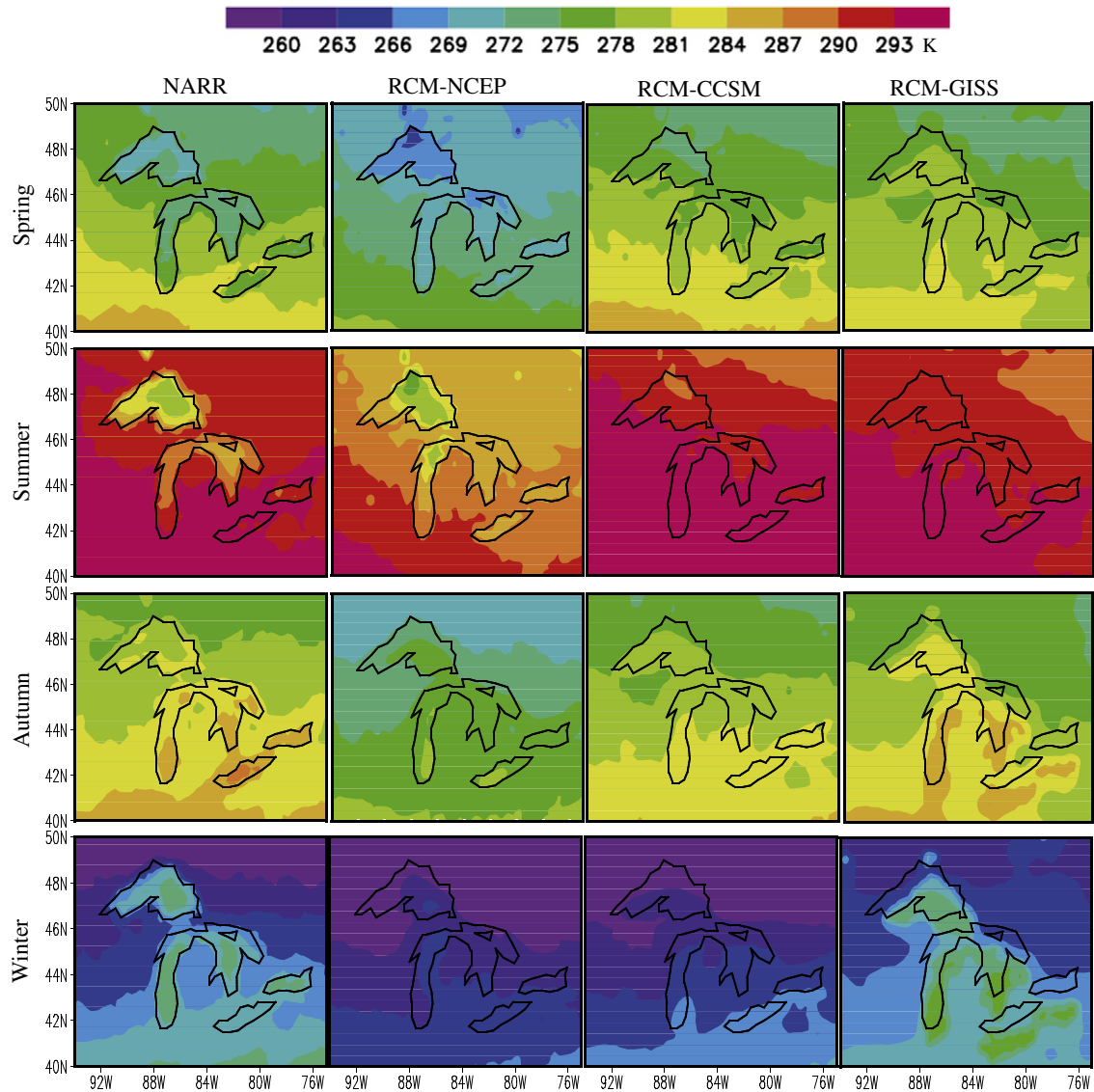


Fig. 1. Spatial distribution of seasonal mean surface air temperature (K) for spring (MAM), summer (JJA), autumn (SON) and winter (DJF).

in combination with the large cold or warm biases of the simulated surface-air temperature implies errors in the simulated static stability of the atmosphere. A less or more stable atmosphere would influence a number of regional or local atmospheric processes such as convection and low-level jet.

Precipitation

Precipitation is one of the most important hydroclimate variables not only because it directly links to natural disasters such as flooding and drought, but also because it controls water resources which in turn affects a large sector of economy such as agriculture and forestry. Fig. 4 shows the spatial distribution of the seasonal mean precipitation over the region. The NARR precipitation patterns exhibit a noticeable change from spring to winter, and a clear influence of the presence of the lakes in the region with suppressed precipitation over the lakes in summer and enhanced precipitation in winter. There is a general south-to-north precipitation gradient, with a higher amount in the south. In the spring and summer seasons, maximum precipitation occurs in the west-southwestern part of the region, while in autumn and winter, the maximum occurs at the southeastern part of the region. The largest spatial variability occurs in summer, when precipitation is more local,

while the smallest variability appears in autumn when the region's precipitation is more influenced by the passage of large-scale systems.

During the spring season, the northern part of the region receives less than 1.5 mm day^{-1} of precipitation and the amount nearly doubles ($\sim 3 \text{ mm day}^{-1}$) in the southern part. This north-south gradient is well simulated by the RCM-NCEP and RCM-GISS, but the simulated amounts are generally larger across the region. The RCM-CCSM fails to produce the maximum in the western and southwestern portions of the region.

Similar to spring, the maximum summer season precipitation in the region also appears in the west-southwest region. There are clear local minima over the Great Lakes. The RCM-NCEP reproduces the general pattern very well, but underestimates the maximum in the west-southwest and slightly overestimates the amount in other parts of the region including the lakes. The two GCM-driven runs are unable to produce the spatial pattern, especially the RCM-CCSM run, and the precipitation amounts are considerably less throughout the region. Because a considerable portion of the summer precipitation is derived from convection processes, the large discrepancy between the simulated and the NARR summer precipitation could be due to the inability to trigger convection in the large-scale environment provided by coarse-resolution GCM simulations and to the possible

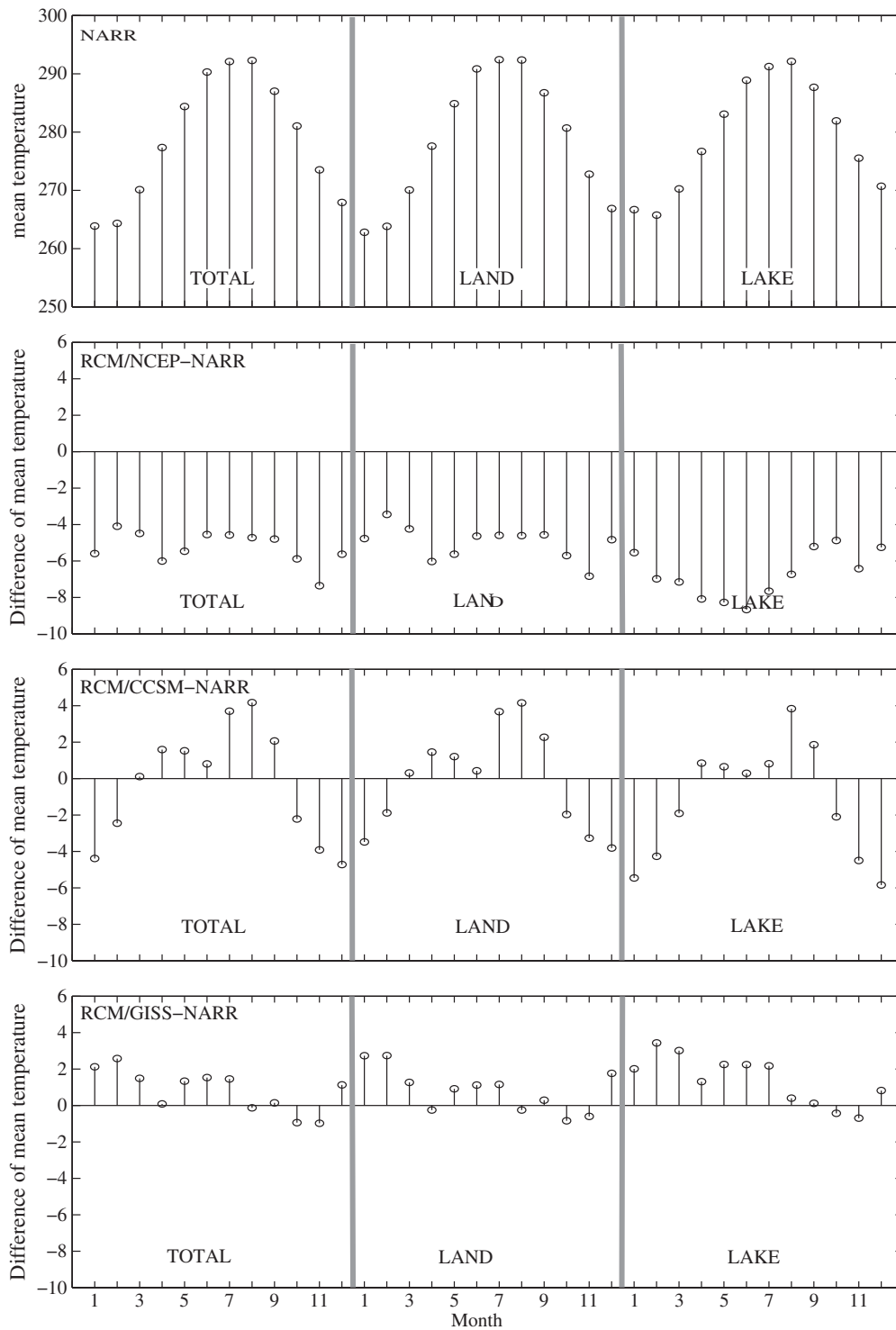


Fig. 2. Monthly mean surface air temperature (K) averaged over the entire Great Lakes region (left), over land (center) and over water (right) for NARR and the temperature differences between NARR and the RCM runs.

disagreement in the formulation of moist convection between the MM5 and the forcing GCMs.

The NARR autumn precipitation is relatively uniform across the region with a weak peak in the southeast. The RCM-NCEP autumn precipitation is also relatively uniform over the region, but instead of local minima over the lakes as in the NARR, local maxima are found over the lakes. The RCM-CCSM and RCM-GISS autumn precipitation is generally lower over the region, except for Lake Superior and Lake Michigan where higher amounts are seen in the RCM-CCSM.

Better agreement between the NARR and two GCM-driven runs occurs in the winter season. A unique feature of the winter season precipitation in the Great Lake region is the enhancement of precipitation on the leeward shores of the Great Lakes when cold air moves across the large body of warmer lake water, creating instability, picking up water vapor, and triggering precipitation as the air converges onto the leeside shore. This so-called lake-effect precipitation, which is clearly shown in the analyzed NARR field, is captured by all three RCM simulations. The precipitation amount,

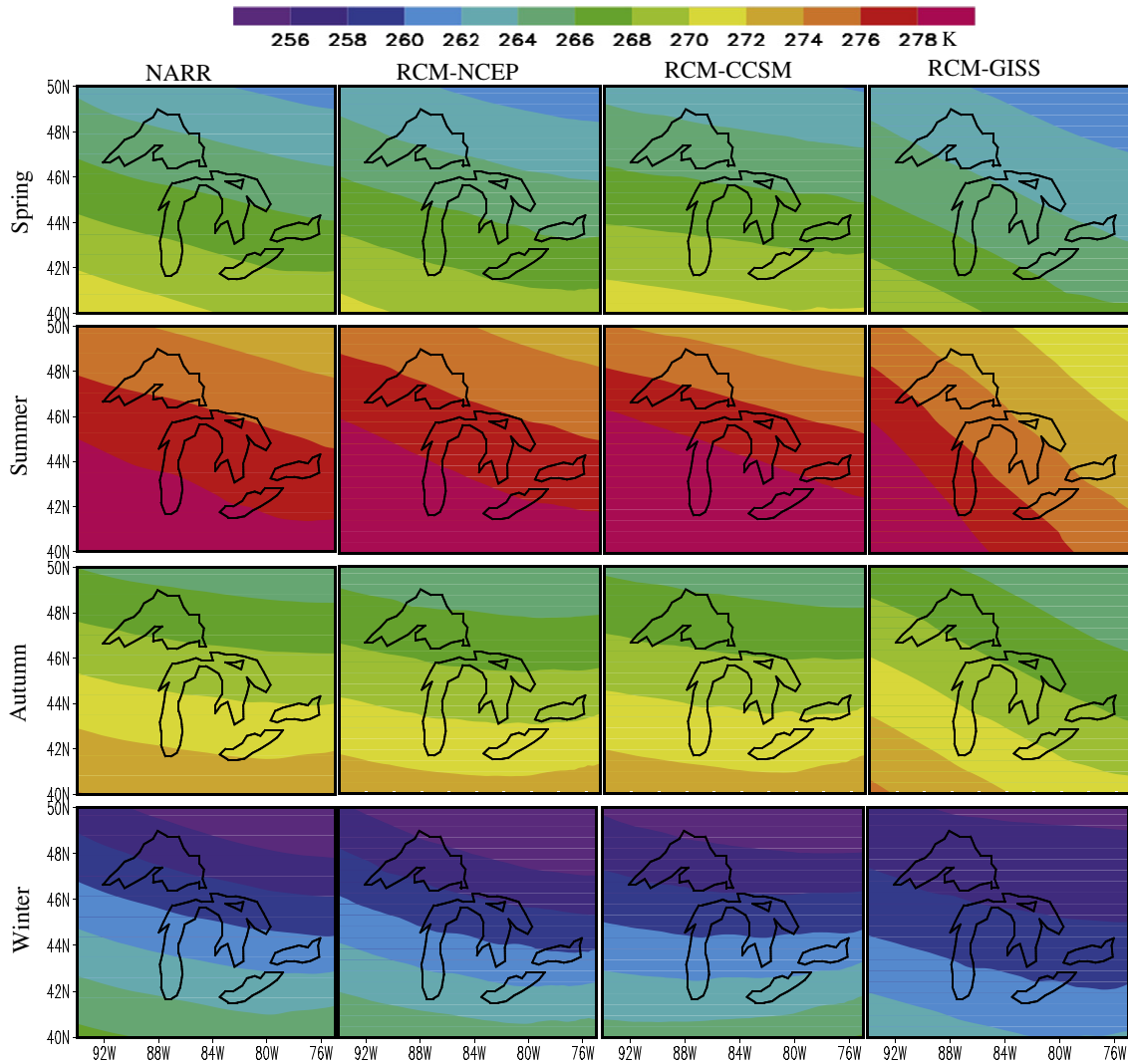


Fig. 3. Spatial distribution of seasonal mean 700 hPa temperature (K).

however, is generally overestimated by the simulations, especially by the RCM-GISS.

Overall, the RCM-NCEP precipitation adequately depicts the spatial distribution and seasonal variation as displayed in the NARR. The simulated precipitation amount is somewhat higher, especially in the northern part of the region, and the maximum summer precipitation in the west-southwestern part of the region is somewhat lower. The spatial distribution and seasonal variability are poorly simulated by the RCM-CCSM, which also significantly underestimates the precipitation amount except for winter when an overestimate occurs. The RCM-GISS is in better agreement with NARR than the RCM-CCSM, but the amount is overestimated in spring and winter, which is reversed in summer and autumn.

The above comparisons reveal the skill of the RCM simulations in producing the spatial patterns and seasonal variability, but they provide little information about the actual errors in the precipitation simulations. To quantify the differences between the NARR and the RCM simulated precipitation amounts and the influence of the lakes on the errors in the simulated precipitation, monthly total precipitation averaged over the Great Lakes region, over the land points of the region, and over the lake points are computed respectively and the results are shown in Fig. 5.

The NARR precipitation exhibits higher amounts in summer with a July maximum, and lower amounts in winter with a minimum in

February. This seasonal cycle is clearly seen over land, but is absent over the lake surfaces where there is large month-to-month variation. The precipitation is greatly enhanced over lake points compared to land points in winter, a result of warmer lake temperatures. The opposite is true for much of the warm season when precipitation is suppressed over lake points because of the cooler temperature over the lakes relative to the surrounding land areas.

RCM-NCEP captures the NARR precipitation seasonal cycle over land and the lack of seasonal variability over water. However, the amount of precipitation is overestimated throughout the year and it is generally worse over the lakes than over land. The overestimation is larger in spring and autumn and small in summer especially over land where the summertime bias is near zero.

The RCM-CCSM simulated monthly precipitation distribution is quite different from that of NARR. Instead of higher amount in summer with an annual maximum in July, RCM-CCSM produces generally lower precipitation and an annual minimum in July. In contrast, the simulated winter season precipitation is much higher than NARR. Over land, the error in RCM-CCSM simulated precipitation exhibits a distinct seasonal dependence with an overestimation in the cold season from November through March and an underestimation in the warm season from April through October. The error is smaller over the lakes and it varies greatly from month to month with no seasonal pattern.

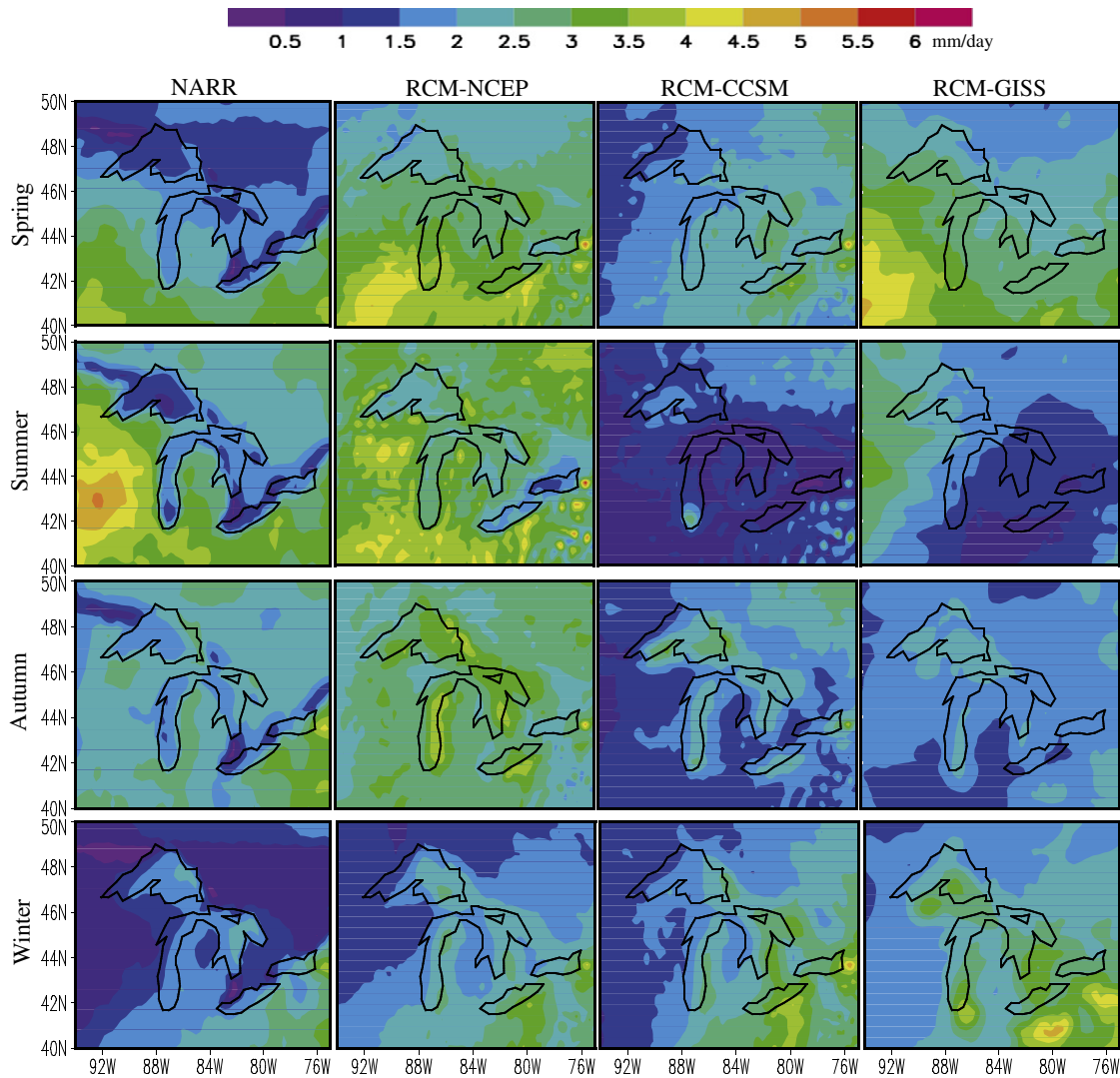


Fig. 4. Spatial distribution of seasonal mean precipitation (mm day^{-1}).

The monthly total precipitation in GCM-GISS is higher than NARR from December through May over both land and water. It is lower from June through October over land, but it varies greatly from month to month during this part of the year over water.

To further understand the contribution of errors in precipitation by convective parameterizations, Fig. 6 shows the comparison of the convective precipitation only. The NARR convective precipitation shows a single peak in July. Compared to the total precipitation in Fig. 5, the summer season precipitation is largely accounted for by convective precipitation. The RCM-NCEP shows exactly the same monthly distribution as NARR, but unlike the total precipitation in the RCM-NCEP that is consistently higher than the NARR, the convective precipitation in the RCM-NCEP is lower than the NARR throughout the year, which suggests that the overestimation of non-convective precipitation is even higher than the overestimation in total precipitation.

The convective precipitation in the RCM-CCSM and the RCM-GISS is smaller for all months, especially during the warm season when the simulated precipitation is less than half of the NARR values, consistent with the underprediction of the total summer season precipitation. The two GCM runs fail to capture the distribution of convective precipitation over an annual cycle. Because the same convective parameterization is used in these simulations, the poorer performance of the two GCM-driven runs in simulating convective

precipitation suggests that the coarse resolution CCSM3 and GISS models are unable to adequately provide the large-scale environments for the development of convection over the region.

Total precipitable water

A comparison of the spatial distribution of the 10-yr seasonal mean precipitable water between NARR and the three RCM simulations is shown in Fig. 7. Similar to surface precipitation, the spatial pattern is dominated by a north–south gradient with a gradual decrease from south to north. The precipitable water also follow similar spatial distribution pattern as the upper-air temperature shown in Fig. 3, which is expected given the non-linear temperature dependency of saturation humidity. The largest spatial variability occurs in summer, as would be expected from more localized convection during the summer season. The winter season pattern exhibits the least spatial variation, consistent with the large-scale nature of the winter precipitation over this region. All three RCM simulations well capture the observed spatial distributions and their seasonal changes. Small differences, however, exist between the simulated and observed values. All RCM simulations appear to have a dry bias of 1–2 mm that occurs over the southernmost part of the region. The dry bias is larger in summer, especially for the RCM-CCSM run, with a bias up to 6 mm.

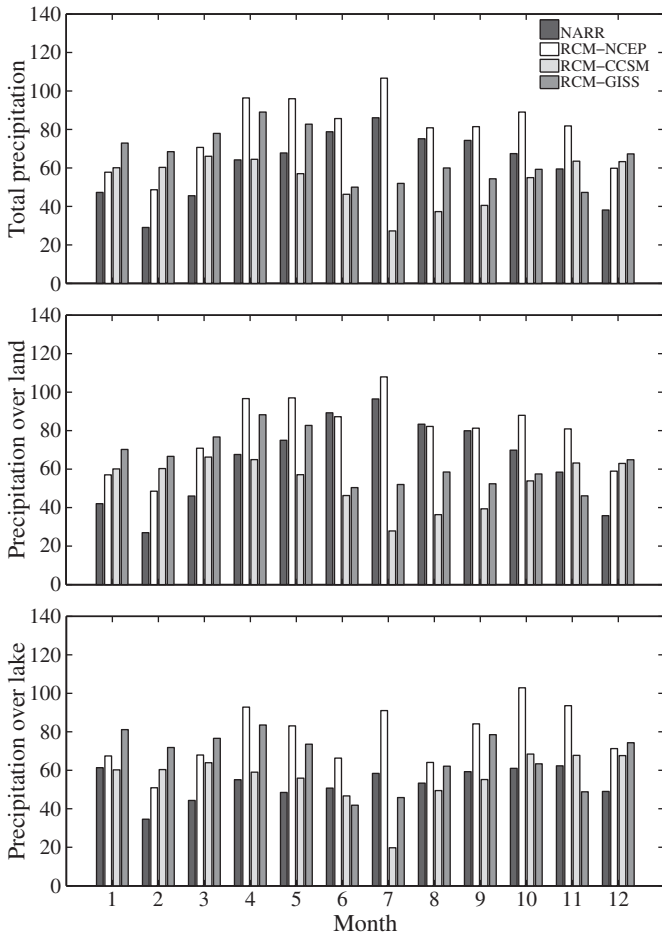


Fig. 5. Monthly total precipitation (mm month⁻¹) averaged over land (middle), over water (bottom), and over both land and water (top) across the Great Lakes region.

Moisture flux

The skill of the RCM in simulating moisture flux is assessed by examining moisture flux across the four lateral boundaries of the

region. According to the Gauss' Theorem, the summation of the fluxes across the four boundaries indicates moisture flux divergence or convergence over the region assuming that there is no flux across the bottom and the top boundaries. A positive value of the total flux through the boundaries indicates a flux divergence over the region and a negative value indicates convergence. Fig. 8 shows the time-height cross section of the total moisture flux across the boundaries or the divergence/convergence of the moisture over the region. In addition, Fig. 8 also shows the meridional component (flux at the northern boundary minus that at the southern boundary) and zonal component (flux at the western boundary minus that at the eastern boundary) of the total moisture flux in order to allow a better examination of the moisture sources and sinks for the region.

The moisture flux in NARR shows a flux divergence in the zonal direction, which is compensated by a convergence in the meridional direction. In the warm season from late April through the end of September, the convergence is slightly larger than the divergence resulting in a net gain of moisture in the lower atmosphere, and the opposite is true during most of the cold season. The moisture flux is mostly confined below 700 hPa with a maximum occurring below 850 hPa. There is a strong vertical gradient in summer, which diminishes in winter.

The RCM-NCEP and RCM-CCSM runs reproduce the time-height distribution of moisture gain/loss and convergence/divergence reasonably well, but both the meridional gain and the zonal loss in the lower atmosphere are larger and the vertical gradients are much stronger than they are in NARR especially in the warm season. However, the extra gain and loss tend to cancel each other, resulting in a net low-level moisture convergence in warm season that is comparable to that of NARR. The RCM-GISS pattern differs significantly from that of NARR. The meridional gain is larger than NARR, similar to the other two RCM runs, and confined almost exclusively to below 800 hPa. The low-level gain is compensated by a loss at upper levels between 800 hPa and 400 hPa in the warm season, a feature that is absent from NARR and the other two RCM runs. The zonal component is much smaller compared to NARR and the two other model runs, with a small lower-level loss during the first half of the year and a small gain in the second half. The total flux is characterized by a stronger low-level convergence for most of the year except for winter, due to somewhat stronger meridional convergence and much weaker zonal divergence.

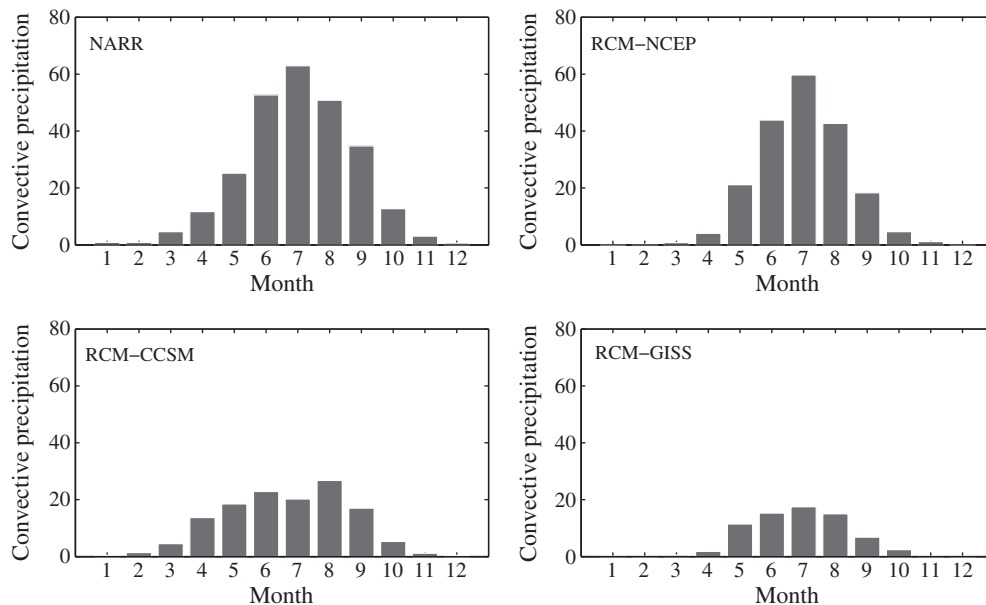


Fig. 6. Monthly total convective precipitation.

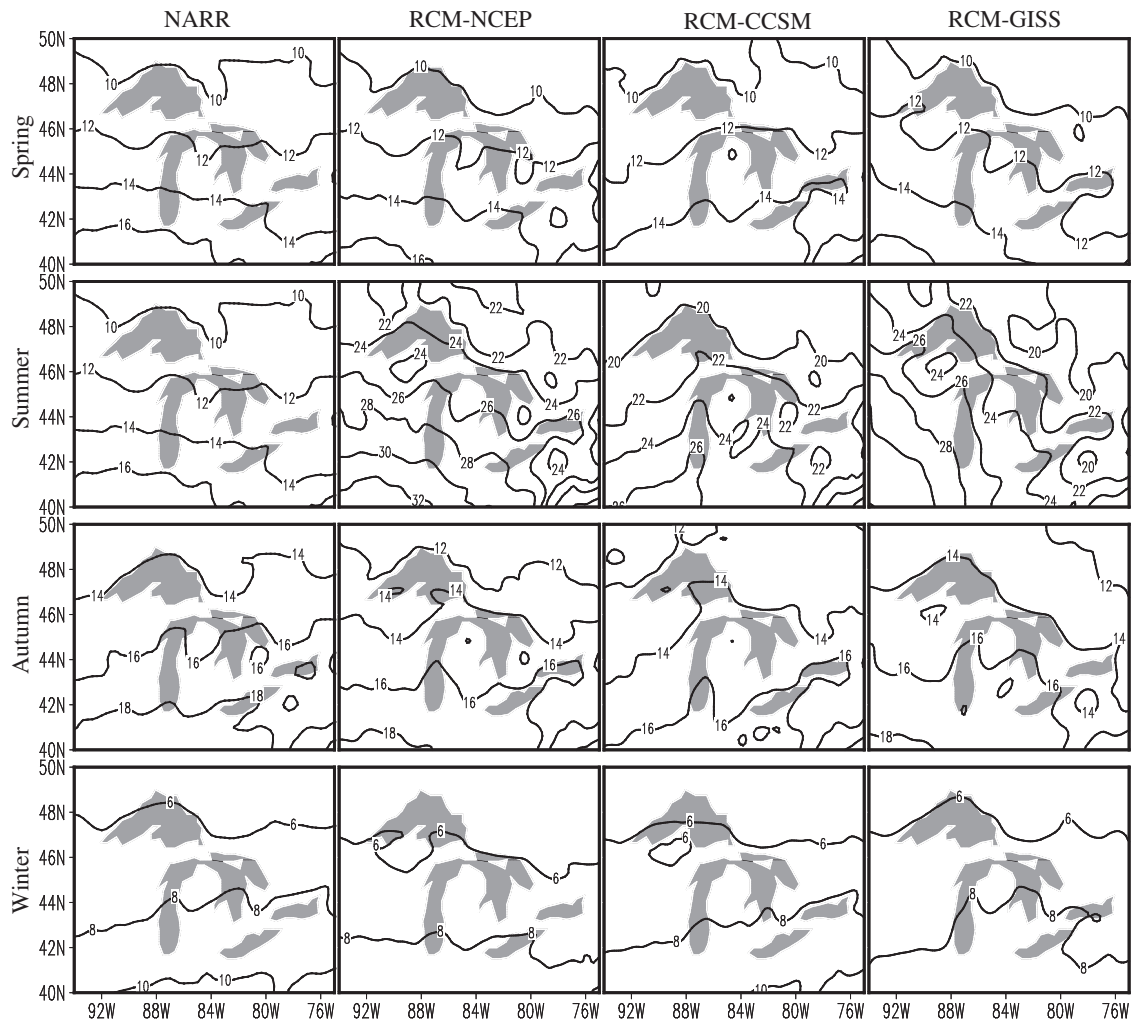


Fig. 7. Spatial distribution of seasonal mean total precipitable water (mm).

To explain the differences between the simulated and observed moisture fluxes, the zonal wind (u), meridional wind (v) and specific humidity (q) components of the moisture flux are examined. Time series of domain-averaged monthly mean winds and specific humidity and their spatial standard deviations are computed, and the results are shown in Fig. 9 for lower (925 hPa) and mid (850 hPa) levels in the atmosphere.

The differences between the RCM and the NARR are consistent at both levels. For all three RCM runs, the simulated means and standard deviations of specific humidity are in better agreement with the NARR data than for the wind components. The RCM-NCEP simulation consistently outperforms the two GCM-driven runs, and the RCM-CCSM run is better than the RCM-GISS run. The observed monthly variability in the zonal and meridional winds and specific humidity is well captured by the RCM-NCEP, but the simulated wind components are consistently over-predicted by $1\text{--}2\text{ m s}^{-1}$. The standard deviations for the zonal wind are comparable to that of the NARR, but the standard deviations for the meridional wind are larger, especially during the warm months. The zonal wind component in the RCM-CCSM run is stronger than the observed for most months, while it is weaker than the observed in the RCM-GISS run. For the meridional component, there is no consistent bias, and the standard deviations are also larger. All model runs reproduce the seasonal variability of specific humidity with a summer maximum and a winter minimum. The RCM-NCEP simulated specific humidity is in excellent agreement with the NARR at low levels (925 hPa), but it is smaller than NARR at

mid level (850 hPa) in summer. The RCM-CCSM simulated specific humidity in summer is underestimated at both levels, while the agreement is good during the other seasons. The RCM-GISS shows a dry summertime bias at 925 hPa, but is in nearly perfect agreement at 850 hPa.

Seasonal variability of moisture flux divergence

Fig. 10 exhibits the spatial distribution of seasonal mean moisture flux divergence/convergence along with wind vectors to show moisture transport at 925 hPa. Since moisture over the Great Lakes region comes primarily from transport by the southerly low-level jet, the analysis region here is extended farther south to capture this transport. At the lower atmosphere south-southwesterly winds prevail, bringing moisture-laden air into the Great Lakes region with more areas of moisture convergence than areas of divergence. Although the spatial patterns of the convergence/divergence vary with season, there are preferred areas of convergence (e.g. Michigan's Lower Peninsula and most of Ontario, Canada) as well as preferred areas of strong divergence (e.g., southwest corner, near south-central boundary, and along the north shore of Lake Superior). The RCM-NCEP and RCM-CCSM successfully simulate the prevailing south-southwesterly flow and, thus, the overall special pattern of moisture convergence/divergence and the seasonal variations. The magnitudes of both convergence and divergence are larger and the areas covered by divergence appear to be somewhat enlarged compared to NARR.

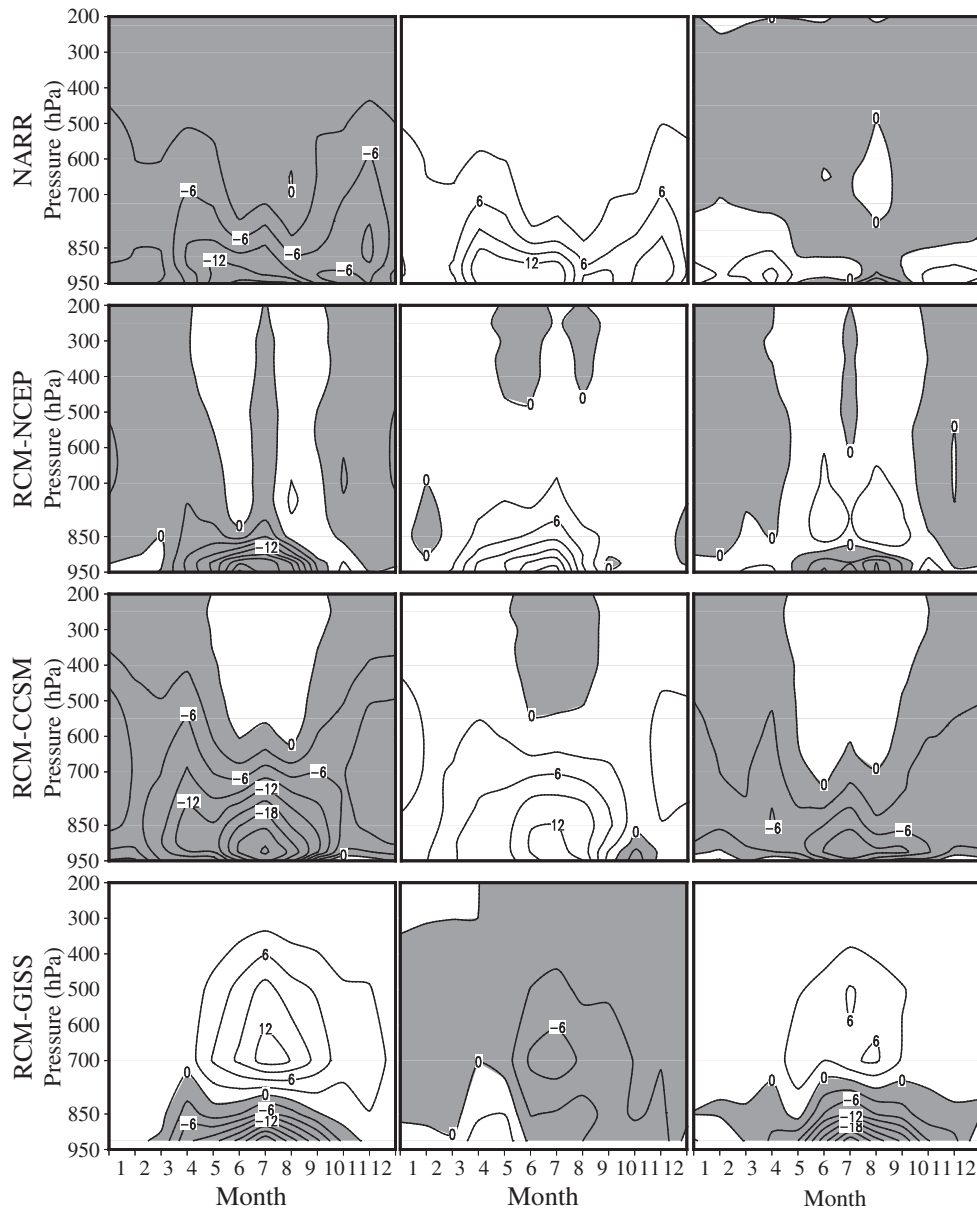


Fig. 8. Time-height cross section of the zonal-average moisture flux through the southern boundary minus that through the northern boundary (left column), the meridional-average moisture flux through the western boundary minus that through the eastern boundary (middle column), and the total flux across all four lateral boundaries (right column) (flux unit: $\text{m s}^{-1} \text{g kg}^{-1}$).

The RCM-GISS failed to capture the prevailing flow especially in summer, and as a result, the simulated moisture flux convergence/divergence patterns are in poor agreement with those of NARR. Similar spatial patterns of convergence/divergence and their seasonal variability are found at 850 hPa level (not shown), but the magnitudes of convergence/divergence are smaller. The differences between NARR and the three RCM runs at 850 hPa are quite similar to the differences at 925 hPa, with RCM-NCEP and RCM-CCSM capturing the dominant flow and the spatial patterns of moisture convergence/divergence and RCM-GISS showing poor agreement.

Vertical structure

To understand how well the model simulations are able to reproduce the observed mean vertical structure of the atmosphere, the RCM-simulated vertical profiles of wind, specific humidity and temperature,

averaged for the region and for all months, are compared to those from the NARR and the results are shown in Fig. 11.

The RCM simulations successfully produce the observed vertical structure of the three variables. The agreement between the simulations and the NARR is better for the specific humidity than wind components. The RCM-NCEP simulation consistently outperforms the two GCM-driven runs, and the RCM-CCSM run is better than the RCM-GISS run. The observed monthly variability of zonal and meridional winds and specific humidity is well captured by the RCM-NCEP, but the simulated wind components are consistently over-predicted by $1\text{--}2 \text{ m s}^{-1}$. The standard deviations for the zonal wind are comparable to that of the NARR, but the standard deviations for the meridional wind are larger, especially in the warm months. The zonal wind component is stronger than observed in the RCM-CCSM run in most months, while it is weaker than the observed in the RCM-GISS run. For the meridional component, there is no consistent bias, and the standard deviation is also larger. All model runs reproduce the seasonal variability of specific

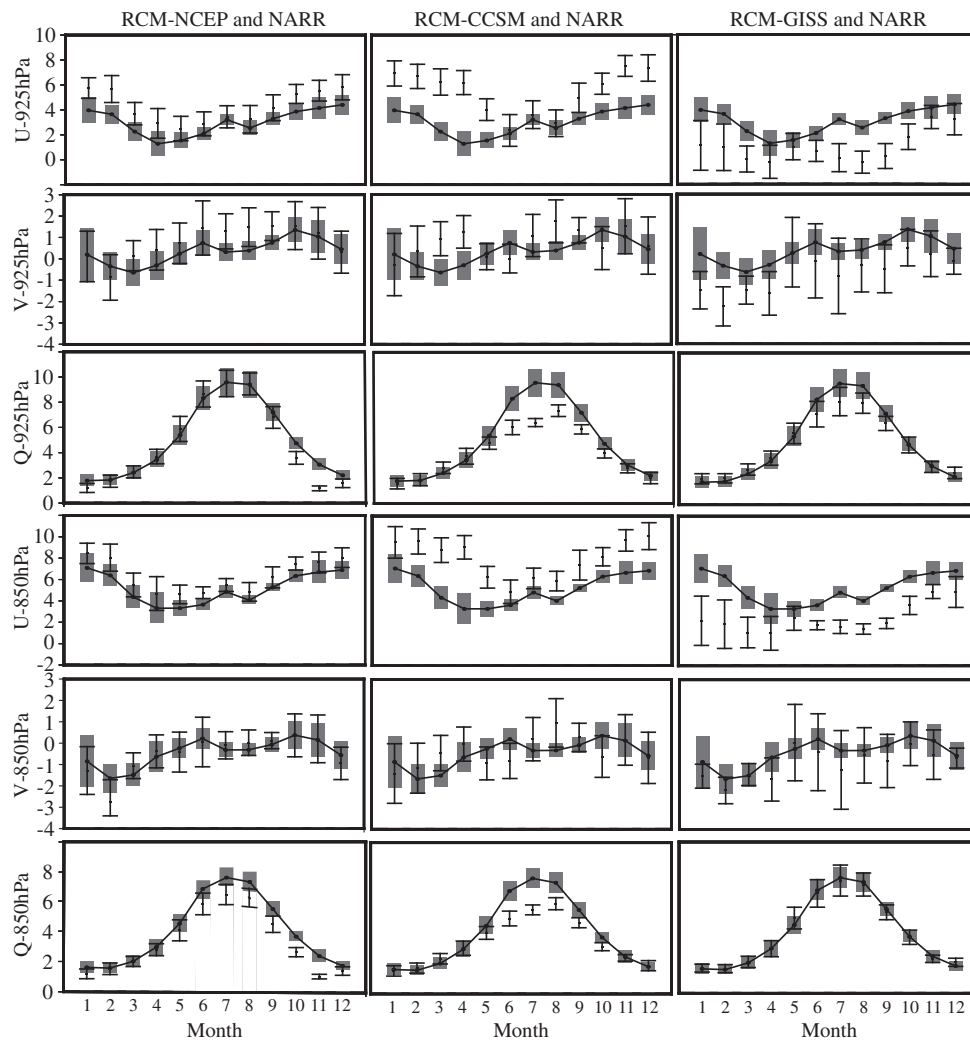


Fig. 9. Regional mean and standard deviation of monthly mean zonal wind (m s^{-1}), meridional wind (m s^{-1}) and specific humidity (g kg^{-1}) at 925 hPa and 850 hPa. The bars denote the regional means and standard deviations from RCMs and the shaded boxes denote the corresponding NARR values.

humidity with a summer maximum and a winter minimum. The RCM-NCEP simulated specific humidity is in excellent agreement with the NARR at the 925 hPa level, is underestimated in summer at the 850 hPa level, and is overestimated in summer at the 500 hPa level. The RCM-CCSM simulated specific humidity is in good agreement with the NARR in all seasons except summer when it is drier at low and mid levels and wetter at high levels. The RCM-GISS simulated specific humidity shows a dry summertime bias at low and upper levels, but is in nearly perfect agreement at 850 hPa.

Discussion

One of the limitations of the current study is the NARR data used for the comparison. As an objectively analyzed gridded dataset that blends operational weather forecast model output with observational data, NARR data are not actual observations and the errors can be large at times and places. As a result, while the current study provides general information on the spatial and temporal distribution of temperature and precipitation biases of RCM simulations over the Great Lakes region, the NARR-based bias estimates may not be as accurate as required by some climate impact studies. Bias estimate based on actual observations would provide the necessary accuracy.

Another limitation of the current study is the relatively short (10 years) averaging period compared to the standard averaging period

of 30 years for climatology. The results should thus be viewed with this caveat in mind. A recent study by Li et al. (2010a, 2010b), which analyzed NARR data for the Great Lake region for the past three decades, revealed no abnormality in both temperature and precipitation for the decade employed in the current study. Generally there are two sources of errors in model simulations related to fast (e.g., clouds) and slow (e.g., land surface) physics. Errors related to fast physics can show up quickly in the simulations. This forms the basis for evaluating climate models using short simulations or weather forecasts (Phillips et al., 2004). Hence we have more confidence in interpreting model errors such as precipitation that are more strongly influenced by fast physics processes, but errors in slow processes will require longer simulations to establish statistical significance. The GCM simulations were free running simulations driven externally only by greenhouse gases and solar variability. Although GCM simulations can vary at interannual and decadal time scales because of natural variability, each simulated year or decade has no direct relationship with the observed year or decade. Hence while it is possible that model errors are due to our short simulation length compared to decadal variability, it is less clear whether the specific time period we chose had any direct implications to the differences we found between the model simulations and the observations. We intend to perform longer simulations in the future using more recent GCM simulations from the Couple Model Intercomparison Project Phase 5 (CMIP5) to investigate this issue.

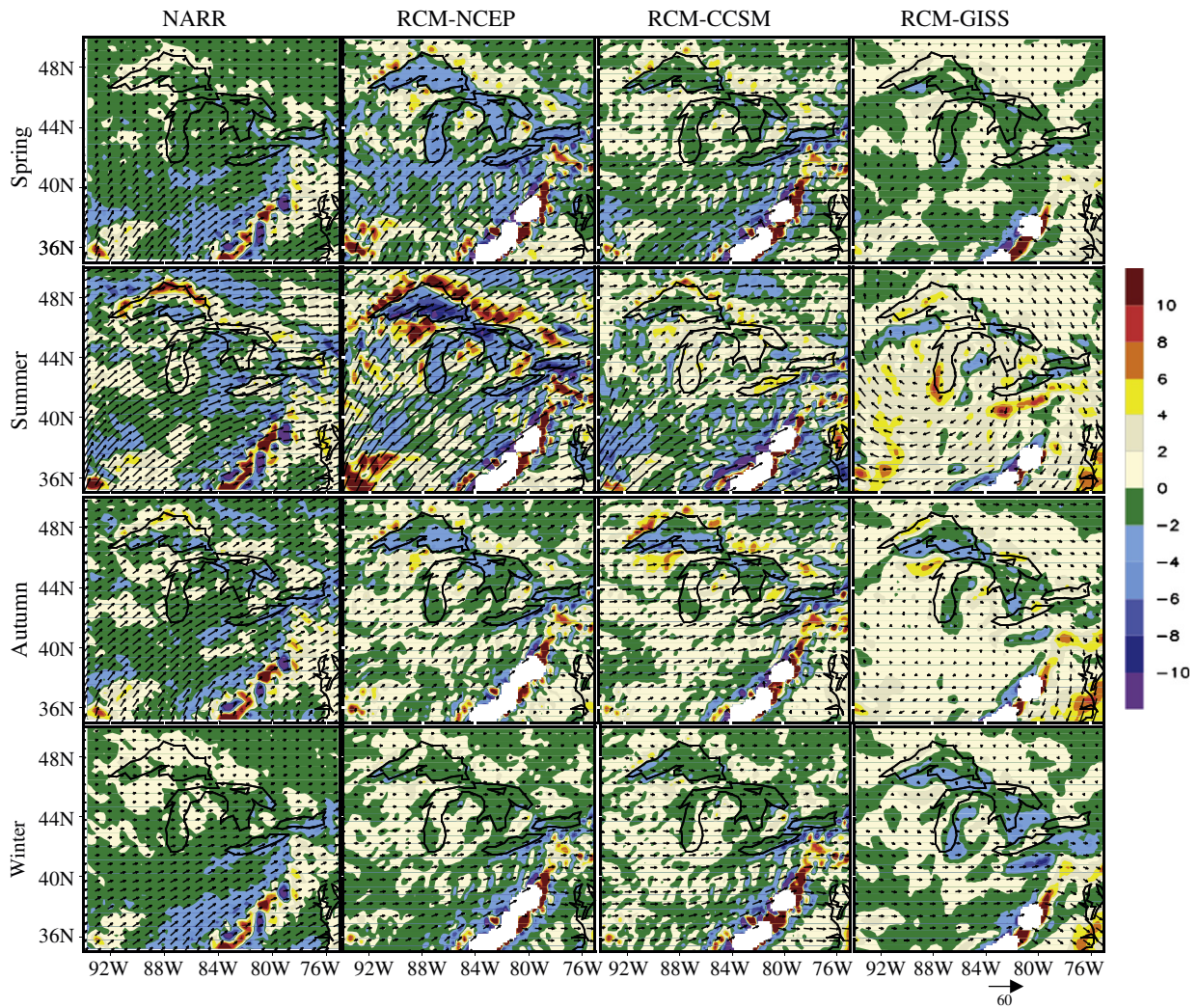


Fig. 10. Spatial distribution of 925 hPa seasonal mean wind vectors (m s^{-1}) and moisture flux convergence (negative values) and divergence (positive values) (unit: $10^{-6} \text{ g cm}^{-2} \text{ hPa}^{-1} \text{ s}^{-1}$).

Summary and conclusion

The performance of RCM simulations over the Great Lakes region of the United States is evaluated. Three 10-year current climate simulations are performed using the MM5 model, with lateral boundary conditions and sea-surface temperature derived from the NCEP reanalysis and the output of the CCSM3 and GISS general circulation models. The results of these simulations are compared to the gridded NARR data with more focus on hydroclimate variables.

For most variables examined, all three simulations are able to capture the spatial distribution across the Great Lakes region as seen in the NARR data. The simulations also reproduce the monthly and seasonal variability. However, differences in the simulated and observed values can be quite large in some areas and in some months. In general, higher accuracy of the simulations is found for the winter season, while larger errors occur during the summer season. The agreement is generally better in the mid- and upper-troposphere than in the lower troposphere.

The reanalysis-constrained simulation (RCM-NCEP) adequately captures the spatial distribution and seasonal variation of the surface-air temperature and precipitation, but it produces a consistent cold and wet bias across the region in all seasons. The wet bias exists despite less convective precipitation in the RCM simulations than in the NARR data, indicating that the overestimation of non-convective precipitation is even larger. The simulated spatial distribution and seasonal variation of moisture flux transport and convergence/divergence are in very good agreement with the observations except for somewhat larger moisture

influx below 850 hPa due mainly to stronger simulated low-level winds. The simulation also captures the observed vertical structure of temperature, humidity, and wind.

The two GCM-driven RCM runs adequately simulate the observed spatial pattern of temperature and its seasonal variability over the region, but produce relatively large errors in hydroclimate variables. Unlike the reanalysis-driven run that produces consistent biases throughout the year, the biases in GCM-driven runs vary with seasons. Both runs underestimate summer precipitation especially the convective precipitation and overestimate cold season precipitation. As a result, the annual cycle of precipitation is reversed from the observed cycle. The failure in simulating annual precipitation cycle has significant implications for applications such as agriculture and forestry that rely heavily on hydroclimate projections for designing climate change adaptation strategies. The RCM-CCSM simulation outperforms the RCM-GISS in simulating moisture flux transport and convergence/divergence patterns over the region, while the RCM-GISS does a somewhat better job in capturing the distribution and magnitudes of air temperature and precipitation at the surface. Given that the configuration and physical parameterizations are identical in all three RCM runs, the poorer performances of the two GCM-driven runs as compared to the reanalysis driven run in simulating precipitation and moisture flux transport point to the importance of boundary conditions for RCM simulations of hydroclimate conditions within the RCM domain.

The climate of the Great Lakes region is uniquely affected by the presence of the large water bodies in the region. Although lake

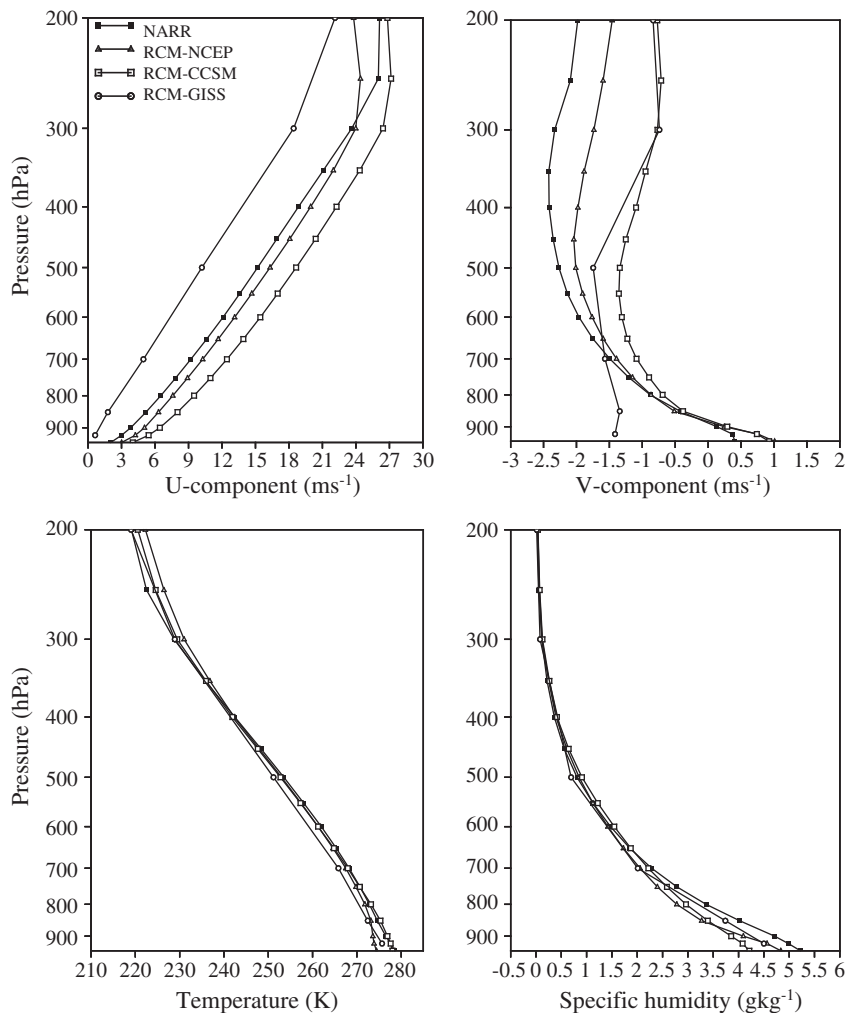


Fig. 11. Annual mean domain-averaged vertical profiles of the u wind component (m s^{-1}), the v wind component (m s^{-1}), specific humidity (g kg^{-1}), and temperature (K).

temperature was simply prescribed based on nearby sea-surface temperature and biases over water are generally larger than over land, all three simulations are capable of capturing the differences between land areas and the lake surfaces. This is because at 36 km grid resolution, the Great Lakes are well resolved so that the influence of the inland water body is captured to some degrees even without the use of a lake model. Most notably, the lake-effect precipitation during winter is captured by all three regional simulations. However, including a lake model to more realistically simulate lake temperature and lake ice will also be important to simulate changes in lake-effect precipitation under global warming.

Overall, the results from the reanalysis-constrained simulation are more realistic than the two GCM-forced runs. This is expected because the lateral boundary conditions derived from the NCEP global reanalysis are closer to reality than the conditions provided by GCM output and errors in the GCM simulations would contribute to the uncertainties in the RCM domain through the imposed lateral boundary conditions. In other words, differences between reanalysis-driven RCM run and NARR reflect errors and uncertainties in the RCM alone, while differences between GCM-driven RCM run and NARR represent errors and uncertainties in both RCM and GCM. Nevertheless, although reanalysis products produce better results when used to drive RCMs, they would not be available for future climate simulations; thus GCM-derived products remain the only tool for future climate projections.

In summary, the results from the current study suggest that RCMs, driven by either reanalysis products or GCM outputs, are capable of

accurately simulating the spatial distribution of temperature and precipitation and their seasonal variability over the Great Lakes region, although biases exist and they vary spatially and seasonally. RCM simulations also depict the influence of the Great Lakes on the climate of the region including lake-effect precipitation by reproducing the land-water contrast and its seasonal changes. However, the relatively large bias values, especially in precipitation and in summer season, point to the importance of de-biasing before RCM products can be employed for climate impact studies for the region. This is especially true for sectors such as agriculture and fruit production that are sensitive to small changes in temperature and precipitation especially during the growing season when the RCM biases are generally larger.

Acknowledgments

This research is supported by the Michigan State University AgBio Research and by the USDA Forest Service Northern Research Station under agreement 07-JV-11242300-138. The work is also partly supported by the PNNL Integrated Regional Earth System Modeling (iRESM) Initiative.

References

- Bates, G.T., Giorgi, F., Hostetler, S.W., 1993. Towards the simulation of the effects of the Great Lakes on regional climate. *Mon. Weather Rev.* 121, 1373–1387.

- Bates, G.T., Hostetler, S.W., Giorgi, F., 1995. Two year simulation of the Great Lakes region with a coupled modeling system. *Mon. Weather Rev.* 123, 1505–1522.
- Castro, C.L., Pielke Sr., R.A., Leoncini, G., 2005. Dynamical downscaling: assessment of value restored and added using the regional atmospheric modeling system (RAMS). *J. Geophys. Res.* 110, D05108. doi:10.1029/2004JD004721.
- Collins, W.D., Bitz, M.C.M., Blackmon, M.L., Bonan, G.B., Bretherton, C.S., Carton, J.A., Chang, P., Doney, S.C., Hack, J.J., Henderson, T.B., Kiehl, J.T., Large, W.G., McKenna, D.S., Santer, B.D., Smith, R.D., 2006. The community climate system model version 3 (CCSM3). *J. Climate* 19, 2122–2143.
- Dudhia, J., 1989. Numerical study of convection observed during the winter monsoon experiment using a mesoscale two-dimensional model. *J. Atmos. Sci.* 46, 3077–3107.
- Duffy, P.B., Arritt, R.W., Coquard, J., Gutowski, W., Han, J., Iorio, J., Kim, J., Leung, L.R., Roads, J., Zeledon, E., 2006. Simulations of present and future climates in the Western United States with four nested regional climate models. *J. Climate* 19, 873–895. doi:10.1175/JCLI3669.1.
- Giorgi, F., Marinucci, M.R., 1996. An investigation of the sensitivity of simulated precipitation to model resolution and its implications for climate studies. *Mon. Weather Rev.* 124, 148–166.
- Giorgi, F., Mearns, L.O., 1999. Introduction to special section: regional climate modeling revisited. *J. Geophys. Res.* 104, 6335–6352.
- Goyette, S., McFarlane, N.A., Flato, G.M., 2000. Application of the Canadian Regional Climate Model to the Laurentian Great Lakes Region: implementation of a lake model. *Atmosphere-Ocean* 38, 481–503.
- Grell, G., Dudhia, J., Stauffer, D.R., 1994. A Description of the Fifth Generation Penn State/NCAR Mesoscale Model (MM5). NCAR Tech. Note., NCAR/TN-398+STR. Nat. Cent. for Atmos. Res., Boulder, CO. 138 pp.
- Gustafson, W.I., Leung, L.R., 2007. Regional downscaling for air quality assessment. *Bull. Am. Meteorol. Soc.* 1215–1227. doi:10.1175/BAMS-88-8-1215.
- Gutowski, W.J., Otieno, F.O., Arritt, R.W., Takle, E.S., Pan, Z., 2004. Diagnosis and attribution of a seasonal precipitation deficit in a U.S. regional climate simulation. *J. Hydrometeorol.* 5, 230–242.
- Hall, N.D., Stuntz, B.B., 2008. Climate change and Great Lakes water resources: avoiding future conflicts with conservation. *Hamline Law Rev.* 31, 641–677.
- Hayhoe, K., Sheridan, S., Kalkstein, L., Greene, S., 2010. Climate change, heat waves, and mortality projections for Chicago. *J. Great Lakes Res.* 36, 65–73.
- Janjic, Z.A., 1990. The step-mountain coordinate: physical package. *Mon. Weather Rev.* 118, 1429–1443.
- Kain, J.S., Fritsch, J.M., 1990. A one-dimensional entraining/detraining plume model and its application in convective parameterization. *J. Atmos. Sci.* 47, 2784–2802.
- Kalnay, E., Kanamitsu, M., Kistler, R., Collins, W., Deaven, D., Gandin, L., Iredell, M., Saha, S., White, G., Woollen, J., Zhu, Y., Chelliah, M., Ebisuzaki, W., Higgins, W., Janowiak, J., Mo, K.C., Ropelewski, C., Wang, J., Leetmaa, A., Reynolds, R., Roy, J., Dennis, J., 1996. The NCEP/NCAR 40-year reanalysis project. *Bull. Am. Meteorol. Soc.* 77, 437–470.
- Karl, T.R., Melillo, J.M., Peterson, T.C., 2009. Global climate change impacts in the United States. U.S. Global Change Research Program Report. 196 pp.
- Kennedy, A., Dong, X., Xi, B., Xie, S., Zhang, Y., Chen, J., 2011. A comparison of MERRA and NARR reanalyses with the DOE ARM SGP data. *J. Climate* 24, 4541–4557. doi:10.1175/2011JCLI3978.1.
- Kim, J., Miller, N.L., Farrara, J.D., Hong, S.Y., 2000. A seasonal precipitation and stream flow hindcast and prediction study in the Western United States during the 1997/98 winter season using a dynamic downscaling system. *J. Hydrometeorol.* 1, 311–329.
- Lettenmaier, D.P., Gan, T.Y., 1990. Hydrologic sensitivities of the Sacramento–San Joaquin River Basin, California, to global warming. *Water Resour. Res.* 26, 69–86.
- Leung, L.R., Ghan, S.J., 1998. Parameterizing subgrid orographic precipitation and surface cover in climate models. *Mon. Weather Rev.* 126, 3271–3291.
- Leung, L.R., Ghan, S.J., 1999. Pacific Northwest climate sensitivity simulated by a regional climate model driven by a GCM. Part II: 2×CO₂ simulations. *J. Climate* 12, 2031–2053.
- Leung, L.R., Qian, Y., 2003. The sensitivity of precipitation and snowpack simulations to model resolution via nesting in regions of complex terrain. *J. Hydrometeorol.* 4, 1025–1043.
- Leung, L.R., Mearns, L.O., Giorgi, F., Wilby, R.L., 2003a. Regional climate research—needs and opportunities. *Bull. Am. Meteorol. Soc.* 84, 89–95.
- Leung, L.R., Qian, Y., Bian, X., 2003b. Hydroclimate of the western United States based on observations and regional climate simulation of 1981–2000. Part I: seasonal statistics. *J. Climate* 16, 1892–1911.
- Li, X., Zhong, S., Bian, X., Heilman, W.E., 2010a. The climate and climate variability of the wind power resources in the Great Lake region of the United States. *J. Geophys. Res.* 115, D18107. doi:10.1029/2009JD013415.
- Li, X., Zhong, S., Bian, X., Heilman, W.E., Luo, Y., Dong, W., 2010b. Hydroclimate and variability in the Great Lakes region as derived from the North American Regional Reanalysis. *J. Geophys. Res.* 115, D12104. doi:10.1029/2009JD012756.
- Liang, X.Z., Li, L., Dai, A.G., Kunkel, K.E., 2004a. Regional climate model simulation of summer precipitation diurnal cycle over the United States. *Geophys. Res. Lett.* 31, L24208. doi:10.1029/2004GL021054.
- Liang, X.Z., Li, L., Kunkel, K.E., Ting, M.F., Wang, J.X.L., 2004b. Regional climate model simulation of U.S. precipitation during 1982–2002. Part I: annual cycle. *J. Climate* 17, 3510–3529.
- Lofgren, B.M., 2004. A model for simulation of the climate and hydrology of the Great Lakes basin. *J. Geophys. Res.* 109, D18108. doi:10.1029/2004JD004602.
- Lofgren, B.M., Quinn, F.H., Clites, A.H., Assel, R.A., Eberhardt, A.J., Luukkonen, C.L., 2002. Evaluation of potential impacts on Great Lakes water resources based on climate scenarios of two GCMs. *J. Great Lakes Res.* 28, 537–554.
- McGregor, J.L., 1997. Regional climate modeling. *Meteorol. Atmos. Phys.* 63, 105–117. doi:10.1007/BF01025367.
- Mearns, L.O., Giorgi, F., McDaniel, L., Shields, C., 1995. Analysis of variability and diurnal range of daily temperature in a nested regional climate model: comparison with observations and doubled CO₂ results. *Clim. Dyn.* 11, 193–209.
- Mesinger, F., DiMego, G., Kalnay, E., Mitchell, K., Shafran, P.C., Ebisuzaki, W., Jovic, D., Woollen, J., Rogers, E., Berbery, E.H., Ek, M.B., Fan, Y., Grumbine, R., Higgins, W., Li, H., Lin, Y., Manikin, G., Parrish, D., Shi, W., 2006. North American Regional Reanalysis. *Bull. Am. Meteorol. Soc.* 87, 343–360.
- Mickley, L.J., Jacob, D.J., Field, B.D., Rind, D., 2004. Effects of future climate change on regional air quality episodes in the United States. *Geophys. Res. Lett.* 31, L24103. doi:10.1029/2004GL021216.2004.
- Miller, N.L., Kim, J., 1996. Numerical prediction of precipitation and river flow over the Russian river watershed during the January 1995 California storms. *Bull. Am. Meteorol. Soc.* 77, 101–105.
- Mortsch, L., Hengeveld, H., Lister, M., Lofgren, B., Quinn, F., Slivitzky, M., Wenger, L., 2000. Climate change impacts on the hydrology of the Great Lakes–St. Lawrence system. *Can. Water Resour.* 25, 153–179.
- Pan, Z., Arritt, R.W., Takle, E.S., Gutowski Jr., W.J., Anderson, C.J., Segal, M., 2004. Altered hydrologic feedback in a warming climate introduces a “warming hole. *Geophys. Res. Lett.* 31, L17109. doi:10.1029/2004GL020528.
- Phillips, Thomas J., et al., 2004. Evaluating parameterizations in general circulation models: climate simulation meets weather prediction. *Bull. Am. Meteorol. Soc.* 85, 1903–1915. doi: http://dx.doi.org/10.1175/BAMS-85-12-1903.
- Reisner, J., Rasmussen, R.J., Bruintjes, R.T., 1998. Explicit forecasting supercooled liquid water in winter storms using the MM5 mesoscale model. *Q. J. R. Meteorol. Soc.* 124B, 1071–1107.
- Rind, D., Lerner, J., Shah, K., Suozzo, R., 1999. Use of on-line tracers as a diagnostic tool in general circulation model development: 2, transport between the troposphere and the stratosphere. *J. Geophys. Res.* 104, 9123–9139.
- Roads, J., Chen, S.-C., Kanamitsu, M., 2003. U.S. regional climate simulations and seasonal forecasts. *J. Geophys. Res.* 108 (D16), 8606. doi:10.1029/2002JD002232.
- Sousounis, P.J., Bisanz, J.M. (Eds.), 2000. Preparing for a Changing Climate: The Potential Consequences of Climate Variability and Change, Great Lakes. Michigan, USA. University of Michigan, Ann Arbor.
- Wang, Y., Leung, L.R., McGregor, J.L., Lee, D.-K., Wang, W.C., Ding, Y., Kumura, F., 2004. Regional climate modeling: progress, challenges, and prospects. *J. Meteorol. Soc. Jpn.* 82, 1599–1628.
- West, G.L., Steenburgh, J.W., Cheng, Y.Y., 2007. Spurious grid-scale precipitation in the North American Regional Reanalysis. *Mon. Weather Rev.* 135, 2168–2184. doi:10.1175/MWR3375.1.